



# Applied Catalysis B: Environmental

journal homepage: [www.elsevier.com/locate/apcatb](http://www.elsevier.com/locate/apcatb)

## Photocatalytic reduction of Cr(VI) over TiO<sub>2</sub>-coated cellulose acetate monolithic structures using solar light

Belisa A. Marinho<sup>a,b,1</sup>, Raquel O. Cristóvão<sup>a,\*1</sup>, Ridha Djellabi<sup>a</sup>, José M. Loureiro<sup>a</sup>, Rui A.R. Boaventura<sup>a</sup>, Vítor J.P. Vilar<sup>a,\*</sup>

<sup>a</sup> Laboratory of Separation and Reaction Engineering, Laboratory of Catalysis and Materials (LSRE-LCM), Department of Chemical Engineering, Faculty of Engineering, University of Porto, Rua do Dr. Roberto Frias, 4200-465, Porto, Portugal

<sup>b</sup> CAPES Foundation, Ministry of Education of Brazil, Brasília, DF 70040-020, Brazil

### ARTICLE INFO

#### Article history:

Received 6 June 2016

Received in revised form

20 September 2016

Accepted 26 September 2016

Available online 28 September 2016

#### Keywords:

Hexavalent chromium reduction

TiO<sub>2</sub> monolithic structures

Heterogeneous photocatalysis

Citric acid

Solar light

### ABSTRACT

The major drawback of TiO<sub>2</sub> based advanced oxidation processes (AOPs) is the use of massive amounts of dispersed nanoparticles that are hard to recover after the water treatment and potentially harmful for humans due to their very small size. The stabilization of the nanoparticles in an adequate inert support is a good strategy to overcome such limitations. In the present work, the photoreduction of Cr(VI) to Cr(III), using citric acid as a hole scavenger, was performed in a tubular photoreactor packed with cellulose acetate monolithic (CAM) structures coated with TiO<sub>2</sub>-P25 thin films by a simple dip coating method and irradiated by simulated or natural solar light. Firstly, the effect of TiO<sub>2</sub> coating layers number on the Cr(VI) photoreduction was analysed. At the optimal amount, the photoreactor provides 0.10 g of TiO<sub>2</sub> per liter of liquid inside the reactor. The support geometry allowed a high surface-area-to-volume ratio, offering an illuminated catalyst surface area per unit of volume inside the reactor of 212 m<sup>2</sup> m<sup>-3</sup>. Following, operating conditions such as pH value, citric acid concentration, irradiation source and initial Cr(VI) concentration were analysed. Several organic species were also tested as hole scavengers. Results indicate reduction rates of 0.07 mmol<sub>Cr(VI)</sub> m<sup>-3</sup> illuminated volume s<sup>-1</sup> and a photonic efficiency of 1.9% during the reduction of 0.02 mM of Cr(VI) with 6 P25 layers and 6.9 mM of citric acid at pH 2.5 and 25 °C. Furthermore, the catalytic bed was reused for 10 consecutive cycles with almost no efficiency decrease after the second cycle, achieving near 100% Cr(VI) removal after 90 min.

© 2016 Elsevier B.V. All rights reserved.

## 1. Introduction

The use of chromium in different industrial activities, such as, electroplating, textile dyeing, leather tanning and metallurgy, results in toxic wastewaters containing chromium species, which must be treated before discharging into receiving water bodies. In natural environments, chromium exists in two major forms: Cr(III) and Cr(VI) [1,2]. Cr(VI) is known as potentially carcinogenic and mutagenic, being in 2015 at the top of 20 substances determined to pose the most significant potential threat to human health by the Agency for Toxic Substances and Disease Registry (ATSDR, USA).

Recently, the photocatalytic reduction of Cr(VI) to Cr(III) using different semiconductors has received considerable attention [3–6]. Due to its high photostability, activity and relatively low cost, TiO<sub>2</sub> has been widely used, both in suspension and in a supported form. In the photocatalytic process, electron (e<sup>-</sup>) and hole (h<sup>+</sup>) pairs are generated due to the absorption of photons with equal or higher energy than the semiconductor bandgap [7]. The generated holes are highly oxidizing, leading to the TiO<sub>2</sub> use on the oxidative degradation of several organic contaminants by hydroxyl radicals. On the other hand, the electrons can be consumed by inorganic species with a reduction potential more positive than the one of the TiO<sub>2</sub> conduction band [8]. In fact, the Cr(VI) reduction has been reported to be successfully achieved by TiO<sub>2</sub> photocatalytic processes [9,10]. However, since the formed holes are not used to reduce Cr(VI), and, in fact, they can produce hydroxyl radicals from water oxidation, the formed Cr(III) can be re-oxidized to Cr(VI). In addition, the electron-hole recombination can also suppress the reaction. To avoid these effects, several organic agents are often

\* Corresponding authors.

E-mail addresses: [raquel.cristovao@fe.up.pt](mailto:raquel.cristovao@fe.up.pt) (R.O. Cristóvão), [vilar@fe.up.pt](mailto:vilar@fe.up.pt) (V.J.P. Vilar).

<sup>1</sup> These authors contributed equally to this work.

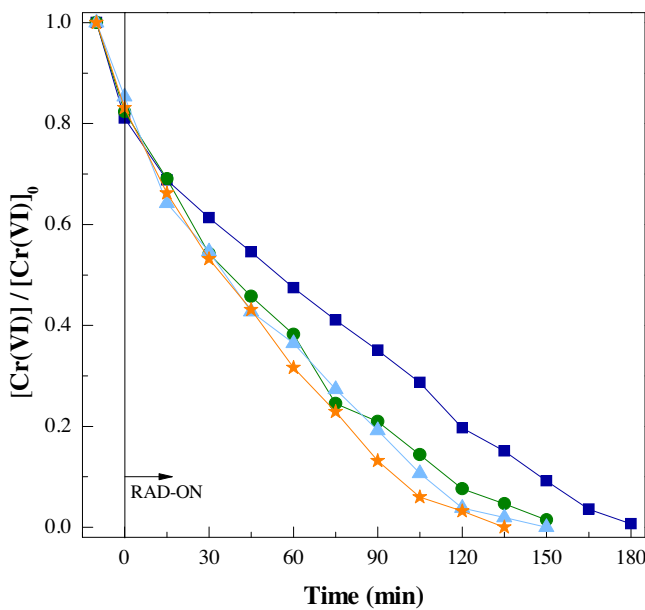


**Fig. 1.** Influence of  $\text{TiO}_2$ -P25 layers number coated in the CAM structures on the Cr(VI) photocatalytic reduction ( $[\text{Cr}(\text{VI})]=0.02 \text{ mM}$ ) by CAM- $\text{TiO}_2$ /UVA-vis/citric acid system at pH 3.0 and  $25^\circ\text{C}$  ( $41 \text{ W}_{\text{UV}} \text{ m}^{-2}$ ); [Citric acid] = 0.6 mM;  $\text{TiO}_2$  layers number = (■) 3, (●) 6, (▲) 9, (★) 12.

added as sacrificial agents, reacting with the  $\cdot\text{OH}$  radicals or holes and hindering the electron-hole recombination, leading, this way, to an enhancement of the reduction process.

Most of the information on water treatment by photocatalytic processes is concerned to the use of dispersed semiconductors. However,  $\text{TiO}_2$  is known to be difficult to separate from the solutions and to limit the penetration depth of UV light [11]. This problem could be avoided through heterogeneous photocatalysis, where inert supports are functionalized with the active nanoparticles, eliminating the need for a post-filtration step and allowing the catalyst reuse as far as its stability is maintained. Supports can be coated with catalyst films by several methods, such as chemical/physical vapour deposition, sputtering or dip coating methods [12]. These methods are normally employed to prepare 2D  $\text{TiO}_2$  thin films stabilized in inert surfaces. Several materials as ceramic tiles, stainless steel, paper, fiberglass and glass were already tested as inert supports [12,13]. Ananpattarchai and Kajitvichyanukul [11] tested a titania-impregnated chitosan/xylan hybrid film in the Cr(VI) removal by adsorption and photocatalysis, proving that the novel sorbent is competitive with  $\text{TiO}_2$  powder. On the other hand, Akkan et al. [14] showed the successful Cr(VI) reduction using  $\text{TiO}_2$  particles immobilized onto biodegradable polymer polycaprolactone, using simple solvent-cast processes. However, despite the several advantages of the heterogeneous reactions, they usually have the mass transfer as a rate-limiting step. In photocatalytic reactions the mass transfer is often quantified by the catalyst surface area per unit reactor volume [15]. This way, thin-walled monolithic structures of cellulose acetate are a promising support alternative since they are UV-transparent, lightweight, inexpensive and easily shaped polymeric materials [12,13,16]. In addition, due to their configuration, cellulose acetate monolithic structures (CAM) allow also a higher irradiated surface area per unit volume inside the reactor, leading to a catalyst efficient exposure to the radiation [17]. Several monolithic catalytic bed reactors were already successfully used in the treatment of aqueous solutions and indoor air by photocatalysis [18,19]. The present work aims to evaluate the performance of CAM structures coated with P25-TiO<sub>2</sub> nanoparticles by a simple dip coating method on the Cr(VI)

**Table 1**  
P25 powder and catalytic bed properties.

$\text{TiO}_2$ – P25 (Evonik®) parameters	Values
Crystal structure	80% anatase, 20% rutile
Crystal size (nm)	25
Surface area ( $\text{m}^2 \text{ g}^{-1}$ )	50
Density ( $\text{g cm}^{-3}$ )	3.9
Eg (eV)	3.25 [16]
$\text{CAM } \rho_{\text{A},\text{P25}} (\text{mg cm}^{-2})$	
3 layers	$1.70 \times 10^{-2}$
6 layers	$4.86 \times 10^{-2}$
9 layers	$6.70 \times 10^{-2}$
12 layers	$9.31 \times 10^{-2}$
CAM film thickness ( $\mu\text{m}$ ) <sup>a</sup>	
3 layers	0.66
6 layers	1.9
9 layers	2.6
12 layers	3.6

<sup>a</sup> Considering a homogeneous film over all walls of the CAM structure.

reduction under simulated solar light with addition of citric acid as sacrificial agent. The effect of several parameters, such as the  $\text{TiO}_2$  amount, solution pH, citric acid concentration, initial chromium concentration, light intensity and the use of other scavengers were studied. Finally, the ability for the photocatalyst to be reused was also analysed.

## 2. Materials and methods

### 2.1. Chemicals

Cr(VI) solutions were prepared from  $\text{K}_2\text{Cr}_2\text{O}_7$  (Merck, purity 99.9%). 1,5-diphenylcarbazide (Merck, purity 98%) was used as colorimetric reagent to determine Cr(VI) concentration.  $\text{TiO}_2$  Degussa P25 powder was supplied by Evonik® and used as delivered, without further modification or purification. Some characteristics of P25 powder provided by the manufacturer are given in Table S1 (see Supplementary material).

TritonTM X-100 ( $t\text{-Oct-C}_6\text{H}_4\text{-(OCH}_2\text{CH}_2)_n\text{OH}$ ,  $n=9\text{--}10$ , Sigma-Aldrich Co. LLC.) was used in the preparation of the  $\text{TiO}_2$ -P25 suspension. Cellulose acetate monolithic (CAM) structures were used as catalyst support. Citric acid monohydrate (VWR Prolabo, purity 98%), oxalic acid dihydrate (VWR Prolabo, purity 98%), maleic acid (Fluka, purity 99%) and disodium EDTA (M&B, purity 98.5%) were used in the photocatalytic experiments. Sulfuric acid (Pronalab, 96%,  $1.84 \text{ g/cm}^3$ ) and sodium hydroxide (Merck) were used for pH adjustment. All samples were filtered through  $0.45 \mu\text{m}$  cellulose acetate membranes (Sartorius) before analysis.

### 2.2. Analytical determinations

Total chromium concentration was determined by atomic absorption spectrometry (AAS, GBC 932 Plus) with a nitrous oxide-acetylene flame, a spectral slit width of  $0.2 \text{ nm}$  and a working current/wavelength of  $6.0 \text{ mA}/357.9 \text{ nm}$ , giving a detection limit ( $D_L$ ) of  $0.08 \text{ mg L}^{-1}$ . The hexavalent chromium concentration was measured by molecular absorption spectrophotometry ( $\lambda = 540 \text{ nm}$ ,  $D_L = 2.05 \mu\text{g L}^{-1}$ ). The procedure followed is based on the formation of a pink complex of Cr(VI) with 1,5-diphenylcarbazide in acid solution, which has an absorbance peak at 540 nm. DOC concentration was directly determined on a Shimadzu TOC-VCSN analyser equipped with an ASI-V auto sampler. Organic acids concentration was measured by HPLC (VWR Hitachi ELITE LaChrom, Merck-Hitach, Tokyo, Japan) equipped with L-2130 pump, L-2200 autosampler, L-2300 column oven and L-2455 DAD. The column REZEX™ ROA (Organic acid H<sup>+</sup> 8%,  $300 \times 7.8 \text{ mm}$ )

**Table 2**

Photonic efficiencies and pseudo-first order kinetic constants for Cr(VI) reduction along with the corresponding coefficient of determination ( $R^2$ ) and residual variance ( $S^2_r$ ).

Experiment	[Cr(VI)] (mM)	TiO <sub>2</sub> (dip's)	[Scavenger] (mM)	pH	T (°C)	$k \times 10^3(\text{min}^{-1})$	$R^2$	$S^2_r \times 10^3(\text{mM})^2$	$r_0 \times 10^3 (\text{mM min}^{-1})$	$\xi (\%)$
Influence of TiO <sub>2</sub> amount										
1.1–3 layers	0.02	3	0.6	3.0	25.0	11.0 ± 0.7	0.951	3	0.150	0.293
1.2–6 layers	0.02	6	0.6	3.0	25.0	13 ± 1	0.941	5	0.226	0.440
1.3–9 layers	0.02	9	0.6	3.0	25.0	17 ± 1	0.974	2	0.244	0.476
1.4–12 layers	0.02	12	0.6	3.0	25.0	18 ± 1	0.972	2	0.238	0.463
1.5 – CAM geometry A	0.02	6	0.6	3.0	25.0	15.7 ± 0.8	0.977	1	0.217	0.422
1.6 – CAM geometry B	0.02	6	0.6	3.0	25.0	14.7 ± 0.8	0.972	2	0.252	0.491
1.7 – CAM geometry C	0.02	6	0.6	3.0	25.0	14.0 ± 0.8	0.978	1	0.212	0.412
1.8 – slurry TiO <sub>2</sub>	0.02	28 <sup>a</sup>	0.6	3.0	25.0	45 ± 7	0.953	6	0.703	1.370
Influence of pH value										
2.1 – pH 2.5	0.02	6	0.6	2.5	25.0	15.7 ± 0.8	0.977	2	0.217	0.422
2.2 – pH 4.0	0.02	6	0.6	4.0	25.0	8.7 ± 0.3	0.984	0.8	0.156	0.305
2.3 – pH 5.0	0.02	6	0.6	5.0	25.0	6.8 ± 0.2	0.980	0.7	0.114	0.223
2.4 – pH 6.0	0.02	6	0.6	6.0	25.0	4.0 ± 0.2	0.955	0.8	0.064	0.124
Influence of citric acid concentration										
3.1–0.2 mM	0.02	6	0.2	2.5	25.0	7.1 ± 0.6	0.929	6	0.128	0.249
3.2–0.4 mM	0.02	6	0.4	2.5	25.0	9.5 ± 0.8	0.938	5	0.158	0.308
3.3–0.6 mM	0.02	6	0.6	2.5	25.0	15.7 ± 0.8	0.977	1	0.217	0.422
3.4–1.2 mM	0.02	6	1.2	2.5	25.0	22 ± 1	0.979	1	0.301	0.587
3.5–2.3 mM	0.02	6	2.3	2.5	25.0	24.4 ± 0.4	0.999	0.1	0.441	0.859
3.6–4.6 mM	0.02	6	4.6	2.5	25.0	44.3 ± 0.6	0.999	0.1	0.683	1.331
3.7–6.9 mM	0.02	6	6.9	2.5	25.0	59 ± 3	0.997	0.4	0.994	1.936
Influence of initial Cr(VI) concentration										
4.1–0.01 mM	0.01	6	6.9	2.5	25.0	47 ± 1	0.998	0.1	0.415	0.808
4.2–0.02 mM	0.02	6	6.9	2.5	25.0	59 ± 3	0.997	0.4	0.994	1.936
4.3–0.03 mM	0.03	6	6.9	2.5	25.0	33 ± 2	0.986	0.2	0.691	1.347
4.4–0.04 mM	0.04	6	6.9	2.5	25.0	22.5 ± 0.6	0.896	30	0.780	1.519
4.5–0.05 mM	0.05	6	6.9	2.5	25.0	8 ± 3	0.971	4	0.309	0.601
4.6–0.06 mM	0.06	6	6.9	2.5	25.0	4.6 ± 0.4	0.826	9	0.198	0.387
4.7–0.06 mM	0.06	6	20.7	2.5	25.0	9.4 ± 0.9	0.926	20	0.306	0.597
Influence of scavenger agent										
5.1 – Maleic acid	0.02	6	6.9	2.5	25.0	7.0 ± 0.7	0.777	4	0.095	0.186
5.2 – Oxalic acid	0.02	6	6.9	2.5	25.0	48 ± 4	0.981	2	0.798	1.555
5.3 – Citric acid	0.02	6	6.9	2.5	25.0	59 ± 3	0.997	0.4	0.994	1.936
5.4 – EDTA	0.02	6	6.9	2.5	25.0	19 ± 7	0.973	2	0.293	0.572
Influence of irradiation source										
6.1 – SUNTEST at 500	0.02	6	6.9	2.5	25.0	3.1 ± 0.1 <sup>b</sup>	0.998	0.3	0.936	1.824
6.2 – SUNTEST at 300	0.02	6	6.9	2.5	25.0	1.3 ± 0.1 <sup>b</sup>	0.971	0.2	0.513	0.566
6.3 – Sunlight	0.02	6	6.9	2.5	–	1.5 ± 0.1 <sup>b</sup>	0.986	0.1	0.487	0.459
Reusability tests										
7.1–1 cycle	0.02	6	6.9	2.5	25.0	45 ± 5	0.971	0.3	0.677	1.319
7.2–2 cycles	0.02	6	6.9	2.5	25.0	27 ± 2	0.976	0.2	0.396	0.771
7.3–3 cycles	0.02	6	6.9	2.5	25.0	25 ± 2	0.962	0.3	0.378	0.737
7.4–4 cycles	0.02	6	6.9	2.5	25.0	25 ± 3	0.935	0.6	0.355	0.691
7.5–5 cycles	0.02	6	6.9	2.5	25.0	27 ± 3	0.958	0.4	0.400	0.780
7.6–6 cycles	0.02	6	6.9	2.5	25.0	29 ± 5	0.914	0.9	0.432	0.841
7.7–7 cycles	0.02	6	6.9	2.5	25.0	23 ± 3	0.924	0.7	0.328	0.639
7.8–8 cycles	0.02	6	6.9	2.5	25.0	22 ± 3	0.920	0.7	0.322	0.627
7.9–9 cycles	0.02	6	6.9	2.5	25.0	22 ± 3	0.921	0.7	0.335	0.653
7.10–10 cycles	0.02	6	6.9	2.5	25.0	26 ± 3	0.948	0.4	0.339	0.661
Reusability tests 2										
8.1–1 cycle	0.02	6	6.9	2.5	25.0	46 ± 3	0.988	0.8	0.785	1.529
8.2–2 cycles	0.02	6	6.9	2.5	25.0	48 ± 4	0.984	0.8	0.817	1.591

<sup>a</sup> mg.<sup>b</sup>  $k \times 10^3 (\text{L kJ})$ .

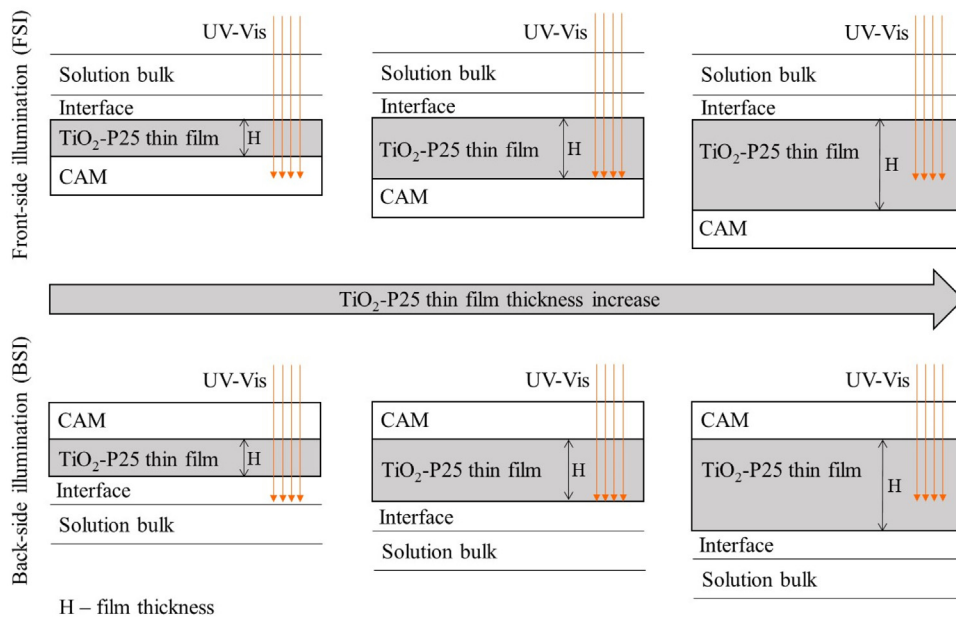


**Fig. 2.** Systems under front-side illumination (FSI) and back-side illumination (BSI) with different TiO<sub>2</sub> thin films thickness.

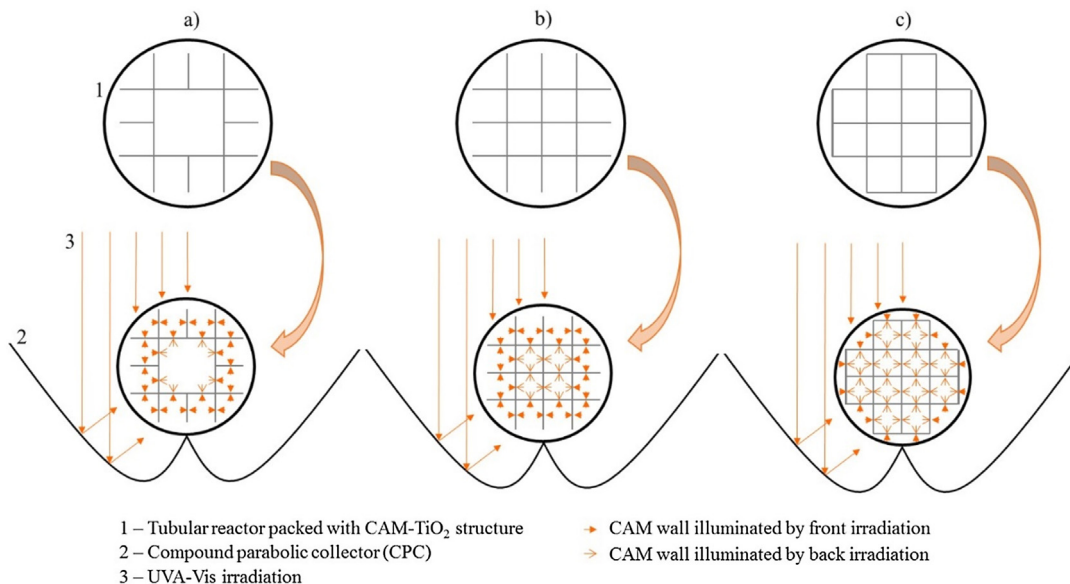


**Fig. 3.** Vertical cut of the tubular reactor packed with the different CAM geometries tested and scheme of the CAM walls irradiated by FSI or BSI.

was operated at 25 °C. The eluent was delivered at a flow rate of 0.5 mL min<sup>-1</sup> in isocratic mode, using sulphuric acid 0.005 N as mobile phase.

### 2.3. Catalyst preparation

CAM structures (TIMax CA50-9/S – length of the cellulose acetate monolith ( $L_{CAM}$ ) = 80 mm; characteristic length of the monolithic channel – hole width ( $d_{ch}^2$ ) = 9 mm × 9 mm; wall thickness of the monolithic channel ( $e_{w, ch}$ ) = 0.1 mm; Wacotech GmbH & Co. KG.) were evenly coated using aqueous suspensions of P25 by the dip-coating method (Dip-Coater RDC 15, Bungard Elektronik GmbH & Co. KG). Several P25 layers (3–12) were deposited by immersing the monolithic structures into an aqueous suspension

at a withdrawal rate of 0.8 mm s<sup>-1</sup>, assuring a thin and uniform film on each substrate surface (samples were dried at 50 °C for 30 min between each layer deposition). Before coating, the monolithic structures were soaked for 1 h with distilled water and alkaline detergent (Derquin LM 01, Panreac Química, S.A.U.), subsequently washed with Milli-Q water, and dried at 50 °C. The photocatalyst aqueous suspension (2 wt.%; two drops of TritonTM X-100) was sonicated for 10 min at 50 kHz in order to better disperse the particles. The TiO<sub>2</sub>-coated monolithic structures were assembled into the tubular photocatalytic reactor for the Cr(VI) reduction studies. The catalytic bed properties are also detailed in Table 1.

The surface morphology of the catalyst film and its chemical composition were characterized by scanning electron microscopy (SEM) coupled with energy dispersive X-ray (EDX) analysis, using

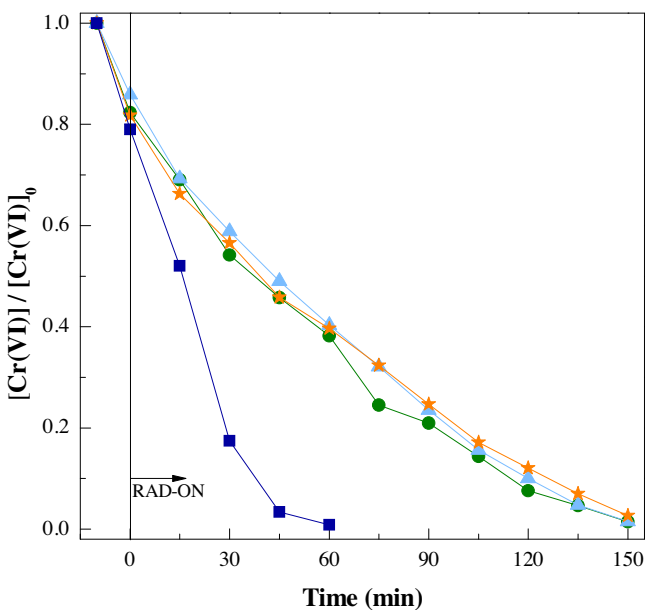


**Fig. 4.** Influence of the CAM-TiO<sub>2</sub>-P25 system and its geometry on the Cr(VI) photo-catalytic reduction ( $[Cr(VI)] = 0.02\text{ mM}$ ) by TiO<sub>2</sub>/UVA-vis/citric acid system at pH 3.0 and 25 °C ( $41\text{ W}_{UV}\text{ m}^{-2}$ ); [Citric acid] = 0.6 mM; Slurry TiO<sub>2</sub> (■); CAM-TiO<sub>2</sub> geometry (●) (a), (▲) (b), (★) (c).

an FEI Quanta 400 FEG ESEM/EDAX Genesis X4M apparatus equipped with a Schottky field emission gun (for optimal spatial resolution). X-ray photoelectron spectroscopy analysis (XPS) was carried out in a Kratos AXIS Ultra HAS equipment and Al monochromator operating at 15 kV (90 W) in hybrid mode. The SEM/EDX and XPS analyses were made at Centro de Materiais da Universidade do Porto (CEMUP), Porto.

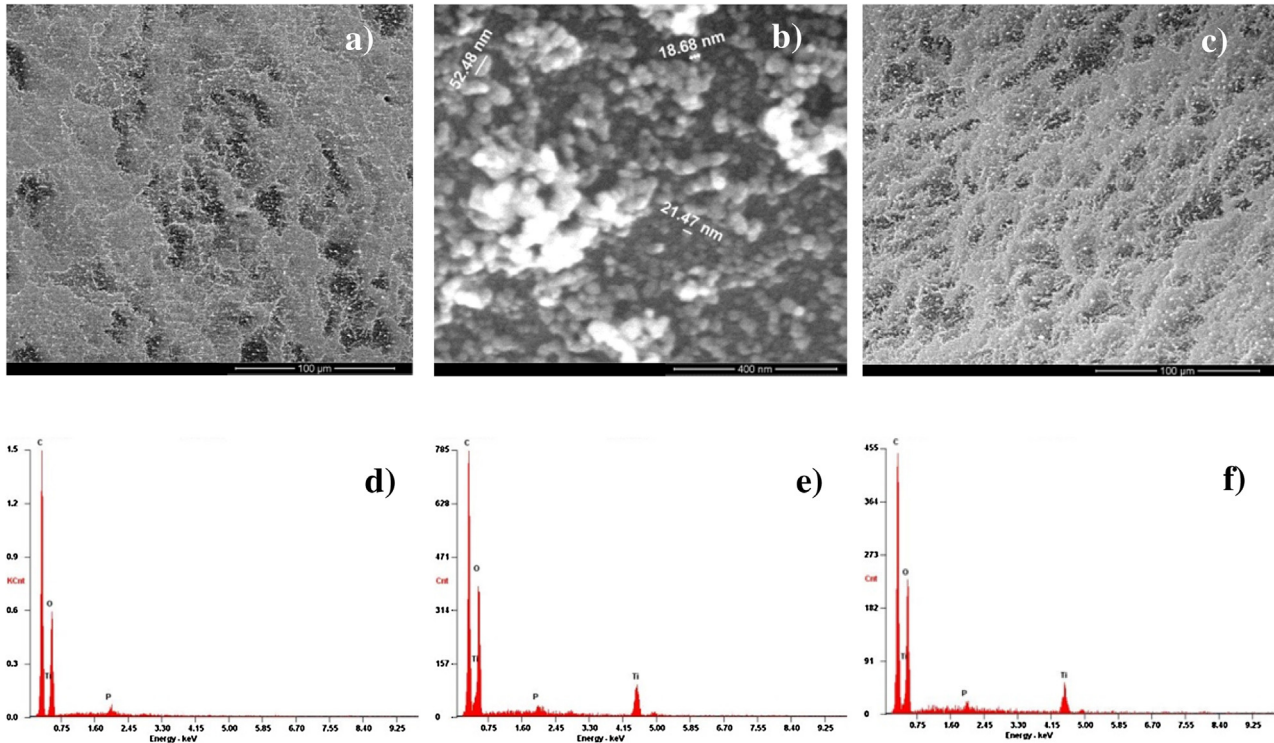


**Fig. 5.** SEM images of (a, b) fresh CAM-TiO<sub>2</sub> sample, (c) used CAM-TiO<sub>2</sub> sample; EDX spectra of (d) natural CAM sample, (e) fresh CAM-TiO<sub>2</sub> sample and (f) used CAM-TiO<sub>2</sub> sample.

## 2.4. Photoreactor

### 2.4.1. Apparatus

The photocatalytic experiments were carried out under simulated solar radiation or natural sunlight in a lab-scale photoreactor already described by Pereira et al. [20].

### 2.4.2. Experimental procedure

The tubular photoreactor was assembled with the monolithic structures coated with TiO<sub>2</sub>-P25 films. The recirculation glass vessel of the lab-scale prototype was filled with 1.5 L of Cr(VI) solution (0.01–0.06 mM), which was pumped to the CPC unit and homogenized by recirculation in the closed system during 15 min in the darkness. The temperature set-point of the refrigerated thermostatic bath was adjusted to keep the intended solution temperature (25 °C). Afterwards, citric acid was added (0.2–6.9 mM) and pH was adjusted in the range 2.5–6.0, using sulphuric acid/sodium hydroxide. Samples were taken after each addition before turning on the solar simulator (SUNTEST). After turning on the SUNTEST the irradiance was set at 300 or 500 W m<sup>-2</sup>, which is equivalent to 27.1 and 41.0 W<sub>UV</sub> m<sup>-2</sup>, respectively, measured in the wavelength range from 280 to 400 nm.

## 2.5. Actinometric experiments

The photonic flux entering the reaction system provided by the UVA-vis lamp (xenon arc lamp 1700 W), installed inside the solar radiation simulator (ATLAS, model SUNTEST XLS), was determined by 2-nitrobenzaldehyde (2-NB) actinometry, adapting the method proposed by Willett and Hites [21] and described in detail by Marinho et al. [22].

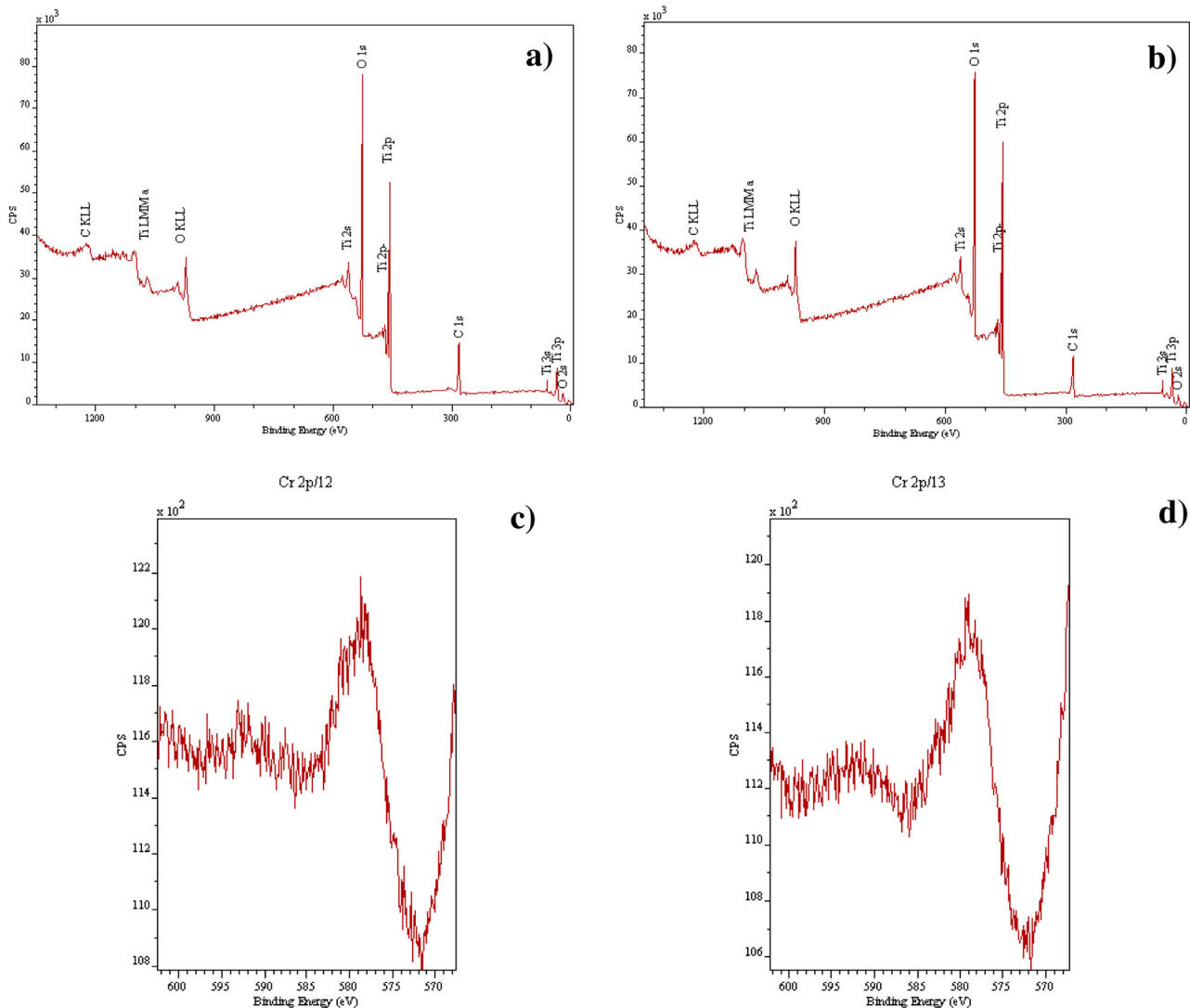


**Fig. 6.** XPS survey of (a) fresh CAM-TiO<sub>2</sub> sample and (b) used CAM-TiO<sub>2</sub> sample; XPS Ti 2p/Cr 2p spectra of (c) fresh CAM-TiO<sub>2</sub> sample and (d) used CAM-TiO<sub>2</sub> sample.

### 3. Results and discussion

#### 3.1. Effect of TiO<sub>2</sub> amount and CAM geometry on the photocatalytic reduction of Cr(VI) by CAM-TiO<sub>2</sub>/UVA-vis/citric acid system

To evaluate the potentiality of the CAM-TiO<sub>2</sub>/UVA-vis/citric acid system and the effect of the TiO<sub>2</sub> amount on the Cr(VI) reduction, a set of photocatalytic experiments was performed using 0.02 mM of Cr(VI), 0.6 mM of citric acid, pH 3.0, 25 °C and varying the number (from 3 to 12) of TiO<sub>2</sub>-P25 thin layers deposited in the CAM structures (Table 1). CAM structures coated with the P25-TiO<sub>2</sub> film showed a good stability (no visible deterioration of CAM surface) under the UVA-vis radiation during a 24 h period. In this case, only water (pH = 3.0) was pumped through the photoreactor packed with the CAM-TiO<sub>2</sub> structures. After this period, the dissolved organic carbon of the solution was negligible. According to the fabricant, the CAM structures are also stable at temperatures between -20 °C and 70 °C. In all the experiments, the solution was firstly homogenized during 15 min in darkness, in order to achieve the system equilibrium. Other authors reported a similar time period (10 min) to this equilibrium phase [23]. Initial tests showed that the removal of 0.02 mM of Cr(VI) by photolysis or by adsorption on

the CAM-TiO<sub>2</sub> structures (density and thickness of 4.86 mg cm<sup>-2</sup> and 1.9 μm, respectively) was negligible during 240 min (data not shown). However, as shown in Fig. 1, the CAM-TiO<sub>2</sub>/UVA-vis/citric acid system is able to achieve the complete reduction of Cr(VI) to Cr(III) in less than 180 min ([Cr(VI)]<sub>0</sub> = 0.02 mM; CAM-TiO<sub>2</sub> structure density of 1.70 mg cm<sup>-2</sup>; TiO<sub>2</sub> film thickness of 0.66 μm).

The Cr(VI) photocatalytic reduction is well described by a pseudo-first order kinetic model [8,9]. Fig. 1 shows that the increase of the number of TiO<sub>2</sub>-P25 thin layers from 3 to 6 led to an increment of the kinetic constant from  $11.0 \times 10^{-3}$  to  $15.7 \times 10^{-3} \text{ min}^{-1}$  (Table 2), achieving the total Cr(VI) reduction, below the detection limit ( $D_L$ ) of the analytical method, after 180 and 150 min, respectively. However, for a higher number of TiO<sub>2</sub> thin layers (9 and 12) the reaction rate remains almost constant, considering the associated error:  $(17 \pm 1) \times 10^{-3}$  and  $(18 \pm 1) \times 10^{-3} \text{ min}^{-1}$ , respectively. The increment of the P25 layers number can result in positive and negative effects: on one hand, it favors the generation of electrons that promote the Cr(VI) reduction, but, on other hand, the CAM structure transparency decreases, hindering the radiation passage which results in a decrease in the reaction rate [23,24]. In fact, the UV photons are emitted from the external side of the photoreactor and the light crosses the borosilicate tube and reaches the TiO<sub>2</sub> thin film immobilized in the external walls of the CAM structure.

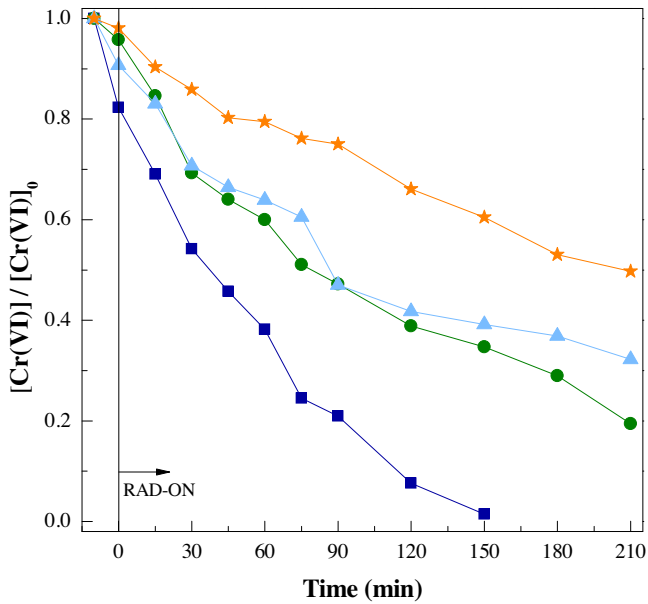


**Fig. 7.** Influence of pH value on the Cr(VI) photocatalytic reduction ( $[Cr(VI)] = 0.02 \text{ mM}$ ) by CAM-TiO<sub>2</sub>/UVA-vis/citric acid system at  $25^\circ\text{C}$  ( $41 \text{ W}_{\text{UV}} \text{ m}^{-2}$ ); [Citric acid] = 0.6 mM; 6 TiO<sub>2</sub>-P25 layers; pH = (■) 2.5, (●) 4.0, (▲) 5.0, (★) 6.0.

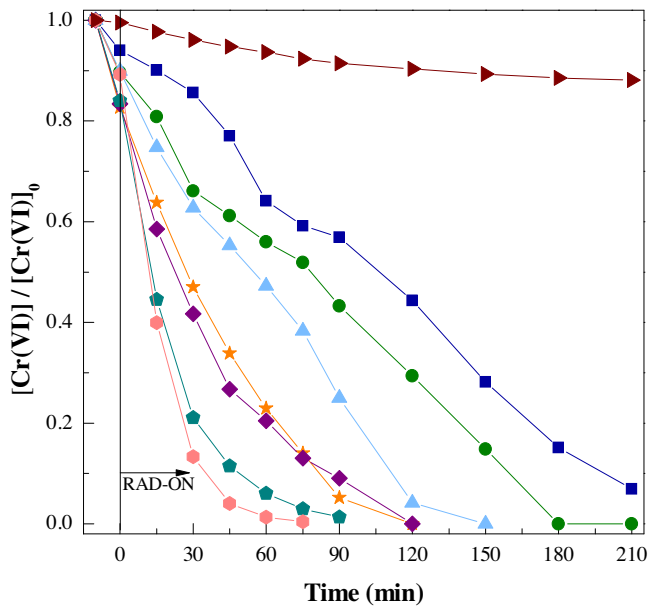


**Fig. 8.** Influence of citric acid concentration on Cr(VI) photocatalytic reduction ( $[Cr(VI)] = 0.02 \text{ mM}$ ) by CAM-TiO<sub>2</sub>/UVA-vis/citric acid system at pH 2.5 and  $25^\circ\text{C}$  ( $41 \text{ W}_{\text{UV}} \text{ m}^{-2}$ ). 6 TiO<sub>2</sub>-P25 layers; Citric acid concentration (mM) = (►) 0.0, (■) 0.2, (●) 0.4, (▲) 0.6, (★) 1.2, (◆) 2.3, (◆) 4.6, (●) 6.9.

In this case, an increase on the catalyst amount (increment of catalyst film thickness) enhances the reaction rate until a point where the light is completely absorbed by the catalyst layer (Fig. 2). After this point, an increase of the catalyst amount does not change the reaction rate, as the diffusional length of the charge carrier to the catalyst-liquid interface will not change (the so called front side illumination (FSI) mechanism). However, in the internal walls of the monolithic structure, the catalyst thin film is illuminated on its backside whereas the pollutant/reactants adsorb on the coating from the other side. In this back-side illumination (BSI) mechanism, the reaction rate will achieve a maximum for a specific catalyst film thickness and a further increase will lower the photocatalytic

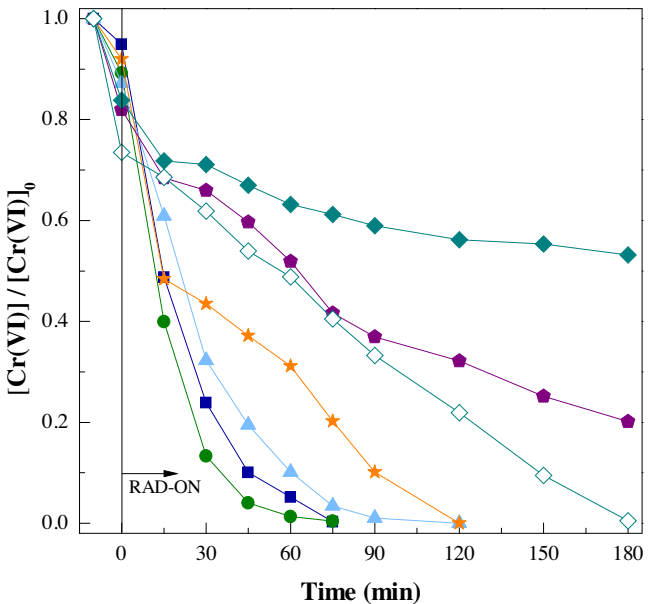


**Fig. 9.** Influence of initial Cr(VI) concentration on its photocatalytic reduction by CAM-TiO<sub>2</sub>/UVA-vis/citric acid system at pH 2.5 and  $25^\circ\text{C}$  ( $41 \text{ W}_{\text{UV}} \text{ m}^{-2}$ ). [Citric acid] = 6.9 mM; 6 TiO<sub>2</sub>-P25 layers;  $[Cr(VI)]_0$  (mM) = (■) 0.01, (●) 0.02, (▲) 0.03, (★) 0.04, (◆) 0.05, (◆) 0.06; (◇)  $[Cr(VI)]_0 = 0.06 \text{ mM}$  and [Citric acid] = 20.7 mM.

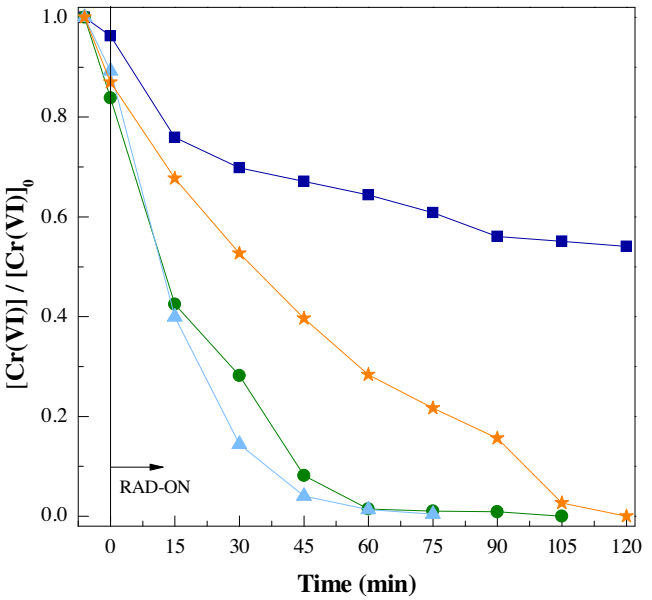


**Fig. 10.** Influence of scavenger agent type on Cr(VI) photocatalytic reduction ( $[Cr(VI)] = 0.02 \text{ mM}$ ) by CAM-TiO<sub>2</sub>/UVA-vis system at pH 2.5 and  $25^\circ\text{C}$  ( $41 \text{ W}_{\text{UV}} \text{ m}^{-2}$ ). [scavenger agent] = 6.9 mM; 6 TiO<sub>2</sub>-P25 layers; scavenger agent = (■) Maleic acid, (●) Oxalic acid, (▲) Citric acid, (★) EDTA.

reaction rate since the charge carriers are generated far from the liquid-catalyst interface and consequently are more susceptible to recombination loss (Fig. 2) [25]. In fact, the light may not reach the catalyst film immobilized in the internal walls of the CAM structure since it can be completely absorbed by the catalyst film deposited in the CAM external walls and by CAM structure itself.

The total chromium concentration decreased only 12% during the reaction, indicating that trivalent chromium has a low affinity to the TiO<sub>2</sub> films, being soluble at the working pH values.

The photonic efficiency ( $\xi$ ) is another important parameter in photocatalysis, defined as the transformed reactant molecules

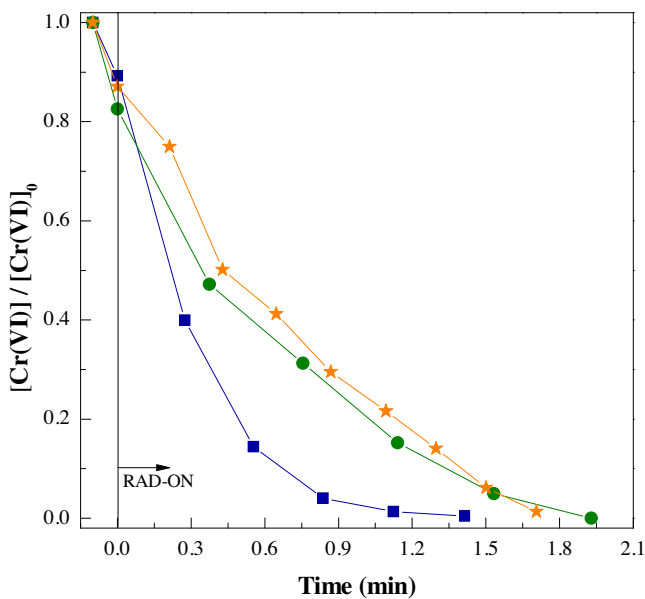


**Fig. 11.** Influence of source of light on Cr(VI) photocatalytic reduction ( $[Cr(VI)] = 0.02 \text{ mM}$ ) by CAM-TiO<sub>2</sub>/UVA-vis/citric acid system at pH 2.5; [Citric acid] = 6.9 mM; 6 TiO<sub>2</sub>-P25 layers; irradiation source = (★) SUNTEST at  $27.1 \text{ W}_{\text{UV}} \text{ m}^{-2}$  (■) SUNTEST at  $41.0 \text{ W}_{\text{UV}} \text{ m}^{-2}$ , (●) Natural sunlight at  $31.0 \text{ W}_{\text{UV}} \text{ m}^{-2}$ .

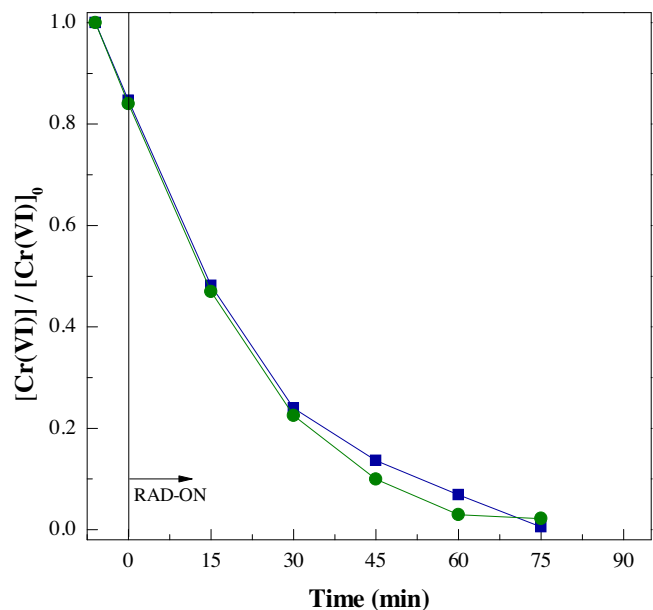


**Fig. 13.** Reuse of CAM-TiO<sub>2</sub> on Cr(VI) photocatalytic reduction ( $[Cr(VI)] = 0.02 \text{ mM}$ ) by CAM-TiO<sub>2</sub>/UVA-vis/citric acid system at pH 2.5 and  $25^\circ\text{C}$  ( $41 \text{ W}_{\text{UV}} \text{ m}^{-2}$ ), considering the CAM structures washing between cycles. [Citric acid] = 6.9 mM; 6 TiO<sub>2</sub>-P25 layers; Cycles number = (■) 1, (●) 2.

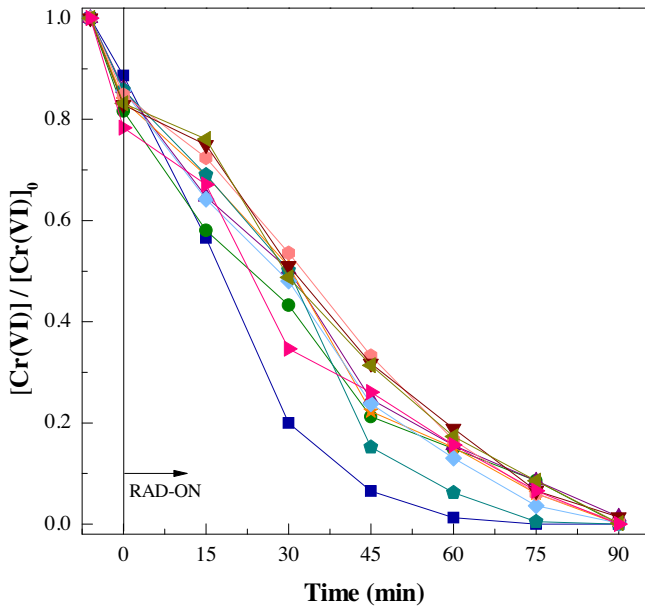


**Fig. 12.** Reuse of CAM-TiO<sub>2</sub> on Cr(VI) photocatalytic reduction ( $[Cr(VI)] = 0.02 \text{ mM}$ ) by CAM-TiO<sub>2</sub>/UVA-vis/citric acid system at pH 2.5 and  $25^\circ\text{C}$  ( $41 \text{ W}_{\text{UV}} \text{ m}^{-2}$ ). [Citric acid] = 6.9 mM; 6 TiO<sub>2</sub>-P25 layers; Cycles number = (■) 1, (●) 2, (▲) 3, (★) 4, (△) 5, (▲) 6, (●) 7, (▼) 8, (▲) 9, (●) 10.

number divided by the number of incident photons on the front window of the reactor [26]:

$$\xi = \frac{\text{rate of reaction}}{\text{incident light intensity}} \quad (1)$$

The determined photonic efficiencies are presented in Table 2 and were calculated from the initial reaction rates ( $r_0$ ), assuming a homogenous illumination of the reactor. As it was observed for the kinetic constant values, the photonic efficiencies using CAM-TiO<sub>2</sub> structures with 12, 9 and 6 layers were found to be similar (0.44,

0.48 and 0.46%, respectively) and higher than the one regarding the use of CAM-TiO<sub>2</sub> structures with only 3 layers (0.29%).

According to these results, monolithic structures coated with 6 P25 layers were used to perform the next experiments. It should be noted that cellulose acetate monoliths contain a large number of walls arranged in several directions where the catalyst is immobilized and through which the aqueous solution to be treated flows, providing, this way, a high surface area-to-volume ratio. In fact, other authors reported that monolithic substrates have 10–100 times higher specific surface areas than plates or beads, considering the same dimensions [17]. Furthermore, the CAM structure can be organized in different geometries in order to present a higher catalyst area per reactor volume. This way, a set of experiments with different CAM-TiO<sub>2</sub> geometries (Fig. 3) with 6 P25 layers (density of  $4.86 \text{ mg cm}^{-2}$  and thickness of  $1.9 \mu\text{m}$  each) was performed using  $0.02 \text{ mM}$  of Cr(VI),  $0.6 \text{ mM}$  of citric acid, pH 3.0 and  $25^\circ\text{C}$ . The geometry presented at Fig. 3(a) (A-CAM) is the same used in the previous experiments with 40 walls coated with TiO<sub>2</sub> thin film. The geometries presented at Fig. 3(b) (B-CAM) and (c) (C-CAM) have 48 and 64 walls, respectively. As shown in Fig. 4, all the three geometries tested are able to achieve the complete reduction of Cr(VI) to Cr(III) in a maximum of 150 min, with similar reaction rates and photonic efficiencies (Table 2). The A-CAM geometry has 32 walls illuminated by FSI and 8 by BSI, the B-CAM geometry has 32 walls illuminated by FSI and 16 by BSI and the C-CAM geometry has 16 walls illuminated by FSI and 48 by BSI. Therefore, using CAM structures with a higher number of walls did not lead to an increase on the reaction rates since light eventually do not reach the catalyst films in the internal walls and FSI is the predominant irradiation mechanism. Consequently, the A-CAM geometry was chosen to perform the next experiments.

In order to compare the Cr(VI) reduction by CAM-TiO<sub>2</sub>/UVA-vis/citric acid system with the TiO<sub>2</sub>/UVA-vis/citric acid in a slurry system, another test was performed using  $28 \text{ mg}$  of TiO<sub>2</sub> in suspension (the same amount coated in the A-CAM-TiO<sub>2</sub> structure). As it is possible to see in Fig. 4, as expected, the reaction rate is higher in the slurry system, mainly due to photons and mass

transfer limitations when using the TiO<sub>2</sub> thin films immobilized the CAM structure [25]. However, even though the use of the immobilized catalyst system leads to a 3-fold decrease in the reaction rate, it has several advantages when compared to slurry systems, as already mentioned above.

At the optimal CAM geometry and TiO<sub>2</sub> film thickness, the photoreactor used in this study provides 0.10 g of TiO<sub>2</sub> per liter of liquid inside the reactor and an illuminated catalyst surface area per unit volume inside the reactor of 212 m<sup>2</sup> m<sup>-3</sup>. Furthermore, it presents a photocatalyst reactivity in combination with the photoreactor of 0.07 mmol<sub>Cr(VI)</sub> m<sup>-3</sup> illuminated volume s<sup>-1</sup> (corresponding to 152 mmol<sub>Cr(VI)</sub> m<sup>-3</sup> illuminated volume kJ<sup>-1</sup>).

The surface morphology and the chemical composition of the CAM-TiO<sub>2</sub> structure (6 TiO<sub>2</sub> layers) were analysed by SEM/EDX before and after use in the Cr(VI) photocatalytic reduction. The SEM images revealed the presence of highly rough surfaces both in samples before (Fig. 5(a)) and after (Fig. 5(c)) use, showing that the structure is maintained during the reaction. This analysis allowed also to see the presence of some particle aggregation and to estimate the particle size, revealing an average range of 18–52 nm (Fig. 5(b)). Lima et al. [27] reported also TiO<sub>2</sub> spheroidal particles of dimensions below 50 nm. Fig. 5(d)–(f) shows the results obtained with EDX analysis of natural CAM (without TiO<sub>2</sub>) and both fresh and used sample (with TiO<sub>2</sub>), respectively. As expected, without TiO<sub>2</sub>, the elemental analysis revealed mainly the presence of C and O atoms related to the acetate monolith composition. In the case of samples coated with TiO<sub>2</sub>, the existence of Ti was also detected, even after its use for Cr(VI) reduction. In addition, some residual P was also detected in all the samples, probably due to the presence of flame retardants in the cellulose acetate monoliths, that are known to contain P [28]. With these EDX analysis it was also possible to check that probably no Cr was adsorbed in the catalyst surface during the reaction. This result is in accordance with the ones obtained by AAS analysis, where a low total Cr concentration decrease was observed (as above mentioned), showing a negligible Cr adsorption in the studied conditions.

However, in order to confirm this conclusion, a more sensitive analysis, that allows the evaluation of chemical position and element oxidation, XPS analysis, was carried out. The results were obtained by a brief spectra analysis with an integrated peaks measurement, without structure patterning, and with a simple background model (Shirley). From the XPS analysis of the CAM structure without TiO<sub>2</sub>, it was possible to identify 2 binding energy peaks related with the CAM composition: C 1s at 285 eV and O 1s at 531 eV (data not shown). As it was expected, the same signals were also observed in the XPS analysis of the CAM samples with TiO<sub>2</sub>, before and after use (Fig. 6(a) and (b)). The characteristic Ti spectra: Ti 2p<sub>3/2</sub>, 2p<sub>1/2</sub> and 2s, with binding energy peaks at 456, 461 and 562 eV, respectively, were observed in both (fresh and used) CAM-TiO<sub>2</sub> samples. These energy peaks are in accordance with the typical Ti spectra reported in the literature [29]. It is known that Cr exhibits binding energy peaks at 574 and 584 eV, corresponding to Cr 2p<sub>3/2</sub> and 2p<sub>1/2</sub> spectra [29]. In the unused CAM-TiO<sub>2</sub> sample spectra (without contact with the chromium solution), it is also possible to observe two peaks in the same position of the ones characteristic of Cr 2p, that correspond to satellite peaks of Ti 2s (Fig. 6(c)). This way, as these 2 peaks are also present in the used CAM-TiO<sub>2</sub> sample spectra (Fig. 6(d)), it is not possible to confirm the Cr presence, since the Cr 2p peaks maybe overlaid by the ones of Ti, leaving the question whether these peaks are only relative to Ti or if there is the presence of some adsorbed chromium. It has to be noted that even if there is some adsorbed chromium, the corresponding amount would be very small, causing no damage/blockage on the catalyst surface.

### 3.2. Effect of pH on the photocatalytic reduction of Cr(VI) by CAM-TiO<sub>2</sub>/UVA-vis/citric acid system

According to the solution pH and chromium concentration, Cr(VI) may exist in several ionic forms (H<sub>2</sub>CrO<sub>4</sub>, HCrO<sub>4</sub><sup>-</sup>, CrO<sub>4</sub><sup>2-</sup>, Cr<sub>2</sub>O<sub>7</sub><sup>2-</sup> and HCr<sub>2</sub>O<sub>7</sub><sup>-</sup>), that require a different number of electrons and protons to achieve the complete reduction to trivalent chromium. Fig. S1 (see Supplementary material) shows the Cr(VI) species distribution as a function of solution pH, for a Cr(VI) concentration of 0.02 mM, being possible to observe that the predominant species for pH values between 2.5 and 6.0 is HCrO<sub>4</sub><sup>-</sup>. As it is possible to see by Eq. (2), this species requires three moles of electrons and seven moles of protons to reduce one mole of hexavalent chromium.

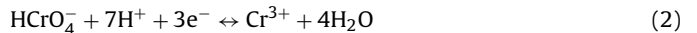
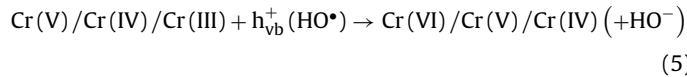
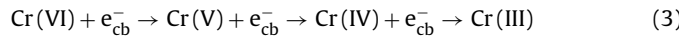


Fig. 7 shows that the solution pH has an important effect on the Cr(VI) photoreduction: the more acidic the pH values are, the higher the respective photoreduction rates. In fact, at solution pH values of 2.5, the total Cr(VI) reduction (below the  $D_L$ ) was achieved in 150 min, whereas at pH 6.0 the Cr(VI) reduction was not totally achieved during the reaction time studied (210 min). Furthermore, a 3.5-fold increase in the photonic efficiency was also verified for lower pH values (pH = 2.5) when compared with the one observed for higher pH values (pH = 6.0) (Table 2). These results are in accordance with the ones described by other authors [30–32]. Ku and Jung [23] reported a pH 4.0 as the pH value where the Cr(VI) adsorption on the TiO<sub>2</sub> surface is maximum; however, they pointed also that, when the stirring speed is kept in a value enough to minimise the mass transfer resistance, the Cr(VI) photoreduction rate-determining step is the surface-reaction after Cr(VI) adsorption on the TiO<sub>2</sub> particles. Nevertheless, this step is known to be more favourable at more acidic pH values. In fact, since the Cr(VI) reduction involves its adsorption on the catalyst surface [33] and at acidic pH values the catalyst surface is protonated as TiOH<sup>+</sup> [34], at those pH values the diffusion of the anionic HCrO<sub>4</sub><sup>-</sup> species to the catalyst surface is enhanced, leading to higher Cr(VI) reduction rates. For alkaline pH values (pH > pH<sub>PZC</sub>; pH<sub>PZC</sub> = 6.5 [35]), the HCrO<sub>4</sub><sup>-</sup> species would be electrostatically repelled by the negatively charged TiO<sub>2</sub> surface, hindering the Cr(VI) reduction [36]. Moreover, as the global reduction reaction consumes protons, the Cr(VI) reduction is also favoured at lower pH values. Finally, despite the Cr(VI) reaction with the TiO<sub>2</sub> conduction band electrons being a thermodynamically feasible process, the Cr(VI)/Cr(III) pair reduction potential is known to decrease 138 mV by increasing the solution pH value in one unit [37,38], and, on the other hand, it is also known that the energy level of the TiO<sub>2</sub> conduction band changes from -0.11 V to -0.46 V as pH varies from 1 to 7 [39]. This way, the higher the solution pH value, the lower the difference between the Cr(VI)/Cr(III) pair and the TiO<sub>2</sub> conduction band redox potentials and, consequently, the lower is the electrons driving force to the Cr(VI). Taking these facts into account, pH values higher than 6.0 were not tested and the optimum pH value found was 2.5.

### 3.3. Effect of citric acid concentration on the photocatalytic reduction of Cr(VI) by CAM-TiO<sub>2</sub>/UVA-vis/citric acid system

The effect of citric acid concentration on the Cr(VI) photoreduction was performed using 0.02 mM of Cr(VI), monolithic structures coated with 6 P25 thin layers, pH 2.5, temperature of 25 °C and varying the citric acid concentration from 0.0 to 6.9 mM. The Cr(VI) chemical reduction by the scavenging agent (without irradiation) in the absence of the photocatalyst was negligible (8% in 210 min, data not shown). However, in the absence of citric acid, the photocatalytic reduction (Eq. (3)) almost stops after 30 min of

reaction, achieving only 10% of Cr(VI) reduction in 210 min (Fig. 8). Some authors have reported the Cr(VI) photocatalytic reduction by successive one-electron steps (Eq. (3)) [1,9]. However, without the presence of a scavenging agent during the reaction, a short-circuiting occurs due to the continuous reduction and reoxidation of chromium species by conduction band electrons and holes or hydroxyl radicals, respectively (Eqs. (3) and (5)) [1,9]:



The citric acid (species D in Eq. (6)) will act as scavenger of the hydroxyl radicals formed during the reactions between the holes and the water (Eq. (4)). Furthermore, that species may also have the function of hole scavenger (Eq. (6)), suppressing the electron–hole recombination. This way, the Cr(III) reoxidation is avoided and the Cr(VI) photoreduction is improved. In fact, the presence of citric acid, as well as the increase of the corresponding concentration, proved to enhance the reaction rate, decreasing significantly the reaction time (Fig. 8). Initially, during the dark period, the Cr(VI) reduction is slightly increased from 6 to 11% with the increment of citric acid concentration from 0.2 to 6.9 mM, respectively. When the solution starts to be irradiated, the gradual increase of citric acid concentration enhanced the Cr(VI) reduction. The highest Cr(VI) reduction rate was observed using a citric acid concentration of 6.9 mM, achieving 96% of reduction after 45 min. On the other hand, with 6.9 mM of citric acid and irradiation, but without TiO<sub>2</sub>, it was observed a Cr(VI) reduction of 40% after 120 min (data not shown), which is in agreement with the reducing nature of the organic acid. As it is possible to observe by Table 2, the pseudo-first order kinetic constant and the photonic efficiency show a 8 fold increase (approximately) when the citric acid concentration increases from 0.2 ( $k = 7.1 \times 10^{-3} \text{ min}^{-1}$ ,  $\xi = 0.25\%$ ) to 6.9 mM ( $k = 59 \times 10^{-3} \text{ min}^{-1}$ ,  $\xi = 1.94\%$ ). This behaviour has been observed in other systems and even higher scavenger concentrations have being reported. Cappelletti et al. [8] reported as optimum scavenger agent dosage 500 mM of isopropyl alcohol for the photocatalytic reduction of 0.3 mM of Cr(VI). According to these results, 6.9 mM of citric acid was chosen as optimal scavenger concentration. At this concentration, the scavenger consumption, as well as the respective dissolved organic carbon (DOC) removal, were also followed along the Cr(VI) reduction reaction. Through the HPLC analysis it was possible to verify that only 3% of citric acid is consumed throughout the entire reaction, having negligible DOC removal during the corresponding time. This result emphasizes the good applicability of the citric acid at this concentration, since it remains in solution during all the reaction, being always available to perform the desired scavenger role. On the other hand, after total Cr(VI) reduction, the remaining organic matter could be oxidized by the photocatalytic process or by a conventional biological post-treatment step. As trivalent chromium precipitation is negligible at the working pH values and the adsorption of trivalent chromium on the catalyst surface is low, the total chromium concentration had no significant changes during the entire reaction time (data not shown).

### 3.4. Effect of initial chromium concentration on the photocatalytic reduction of Cr(VI) by CAM-TiO<sub>2</sub>/UVA-vis/citric acid system

The effect of initial Cr(VI) concentration on its photoreduction was evaluated by varying the corresponding concentration from 0.01 to 0.06 mM at pH 2.5 and 25 °C, using 6.9 mM of citric acid. As depicted in Fig. 9, the Cr(VI) reduction efficiency gradually decreases with the increase of the respective initial concentration. For the lowest concentrations studied (0.01 and 0.02 mM) the Cr(VI) total reduction is achieved after 75 min of reaction. However, for Cr(VI) initial concentrations of 0.03 and 0.04 mM, the total reduction is only achieved after 120 min, and increasing the concentration to 0.05 mM, the reduction is only completed after 180 min, under the same photoreduction conditions. In turn, the total reduction of 0.06 mM of Cr(VI) is not even achieved during the reaction time considered, reaching only about 50% after 180 min.

**Table 2** shows that the reaction rate decreased from  $59 \times 10^{-3}$  to  $47 \times 10^{-3} \text{ min}^{-1}$  with the decrease of Cr(VI) initial concentration from 0.02 to 0.01 mM. This can be attributed to the TiO<sub>2</sub> catalyst surface saturation in the presence of extremely high citric acid amounts regarding the Cr(VI) concentration used. Citric acid molecules can hinder the Cr(VI) molecules to reach the catalyst surface or even block it from receiving radiation, decreasing, consequently, the Cr(VI) photocatalytic reduction efficiency. Moreover, the reaction rate also decreased from  $59 \times 10^{-3}$  to  $4.6 \times 10^{-3} \text{ min}^{-1}$  with the increase of Cr(VI) initial concentration from 0.02 to 0.06 mM. Other authors, working with TiO<sub>2</sub> in suspension, have already reported the same behaviour: triplicating the initial Cr(VI) concentration, they observed a 3 fold decrease in the kinetic constant (from  $37 \times 10^{-3}$  to  $13 \times 10^{-3} \text{ min}^{-1}$ ) [23]. Despite the pseudo-first-order kinetic constant is independent of the Cr(VI) concentration, in this case, there is a competition between Cr(VI) and citric acid species for the binding sites on the catalyst surface. The negative effect of higher Cr(VI) initial concentrations could also be attributed to the catalyst surface saturation, but now by the Cr(VI) molecules, avoiding the binding of the citric acid species. Moreover, it is also possible to occur the generation of a screen effect, where the Cr(VI) species could make more difficult for the light to reach the P25 surface, decreasing, consequently, the Cr(VI) photocatalytic reduction efficiency. A decrease on the photonic efficiency was also observed, from 1.94 to 0.39%, comparing the experiments with Cr(VI) initial concentrations of 0.02 and 0.06 mM, respectively. However, as can be seen from Table 2, increasing the citric acid and the initial Cr(VI) concentrations in the same proportion (i.e., using 20.7 mM of citric acid for an initial Cr(VI) concentration of 0.06 mM), the reaction rate was increased by a factor of 2, achieving the total Cr(VI) reduction in 180 min (Fig. 9). This means that, although higher Cr(VI) concentrations take longer times to be reduced due to the reasons mentioned above, the ratio between the initial Cr(VI) concentration and the respective scavenger agent optimal concentration should always be maintained. Additionally, it was verified that the total chromium concentration remained almost constant over the entire reaction time, meaning that the Cr(III) adsorption by the photocatalyst was negligible at the studied conditions.

### 3.5. Effect of scavenger agent type on the photocatalytic reduction of Cr(VI) by CAM-TiO<sub>2</sub>/UVA-vis system

To evaluate the effect of the scavenger agent type on the toxic hexavalent chromium (0.02 mM) reduction to the less toxic trivalent chromium using the heterogeneous TiO<sub>2</sub> photocatalytic system (CAM structures coated with 6 P25 thin layers), several organic acids with different characteristics were tested at pH 2.5

and 25 °C. Beyond citric acid, EDTA, oxalic and maleic acids were evaluated as sacrificial agents at a concentration of 6.9 mM.

The tested scavenging agents exhibited different effects on the reduction of Cr(VI) over TiO<sub>2</sub> both under and without simulated solar light. During the equilibrium period (without irradiation), but in the presence of organic acids, a Cr(VI) reduction of about 5% is observed with maleic acid in 120 min of reaction, while reductions of 11, 13 and 16% were observed in the presence of citric acid, EDTA and oxalic acid, respectively, during the same reaction time. The best result using irradiation was achieved with citric acid, attaining total Cr(VI) reduction (below the  $D_L$  of the method) after 75 min of reaction. In the presence of oxalic acid and EDTA, the Cr(VI) total reduction was achieved after 105 and 120 min of reaction, respectively. With maleic acid as scavenging agent, the complete reduction of Cr(VI) was not achieved during the reaction time period studied (Fig. 10).

The pseudo-first order kinetic constant,  $k$ , as well as the photonic efficiency increased in the following order: maleic acid < EDTA < oxalic acid < citric acid. It can be seen from Table 2 that  $k$  and photonic efficiency values increased by a factor of 8 and 10, respectively, when comparing maleic and citric acid as sacrificial agents. As the photocatalytic reduction of Cr(VI) occurs on the catalyst surface rather than in the bulk solution, only the scavenging agents that efficiently adsorb on the TiO<sub>2</sub> surface are effective [40]. Actually, low molecular weight carboxylic acids can adsorb on the TiO<sub>2</sub> surface and promote the Cr(VI) reduction by a charge-transfer-complex (CTC)-mediated process using, also, the visible light to initiate a direct electron transfer from the surface-complexed organics to the TiO<sub>2</sub> conduction band and then to the Cr(VI) [41]. Franch et al. [42] reported that at pH values lower than the point of zero charge of TiO<sub>2</sub> (6.5), the adsorption of maleic acid onto TiO<sub>2</sub> particles is, in fact, a key feature for its photocatalytic degradation. However, therefore, a cis-trans isomerization induced by the interaction between the adsorbed diacid and the semiconductor surface occurs. As this isomerism is proposed to occur by way of reductive electron transfer to the adsorbed molecule [43], maleic acid will act as an electron acceptor, parallel to Cr(VI), explaining the lower Cr(VI) reduction results attained. On the other hand, a plausible reason for the result achieved with EDTA acting as scavenging agent may be the interference effect of the adsorbed organic molecule that has higher molecular size and adsorption efficiency than the Cr(VI) to the surface of TiO<sub>2</sub>. In turn, using citric or oxalic acid, the formation of highly reducing radicals, such as HCOO<sup>•</sup> occurs, enabling the Cr(VI) photoreduction to shift from the initial direct surface-mediated reaction to an indirect radical-mediated reaction, intensifying the whole heterogeneous photocatalysis [31].

In addition, to explain the differences observed between the results with citric and oxalic acids, two other properties associated with intramolecular electron transfer are important on the Cr(VI) reduction: the energy of the highest occupied molecular orbital ( $E_{HOMO}$ ) and the adiabatic ionization potential (AIP). Wang et al. [41] reported that a higher energy of the highest occupied molecular orbital or a lower ionization potential of the organic acid is favourable to electron transfer within the TiO<sub>2</sub>-organic acid complex, thereby accelerating the photoreduction of Cr(VI). In fact, as the energy gap between the conduction band of TiO<sub>2</sub> and the highest occupied molecular orbital of the organic acid are increased, the photo-induced electron transfer driving force within the TiO<sub>2</sub>-organic acid complexes is also increased. On the other hand, a higher ionization potential makes the removal of an outermost electron more difficult. This way, the better result achieved with the citric acid could be explained by the higher value of  $E_{HOMO}$  (-0.2441 and -0.2520 a.u., for citric and oxalic acids, respectively

[41]) and the respective lower AIP value (0.3318 and 0.3710 a.u., for citric and oxalic acids, respectively [41]).

### 3.6. Effect of irradiation intensity on the photocatalytic reduction of Cr(VI) by CAM-TiO<sub>2</sub>/UVA-vis/citric acid system

The Cr(VI) photoreduction by TiO<sub>2</sub>/UVA-vis/citric acid system changes according to the wavelength and intensity of the light source. Beyond that, the solar light irradiance can vary during the day, according to seasons of the year, location and weather conditions. To clarify in detail the effect of light source wavelength and intensity on the Cr(VI) photocatalytic reduction, experiments with 0.02 mM of Cr(VI) using monolithic structures coated with 6 P25 thin layers and a citric acid concentration of 6.9 mM were performed at pH 2.5 and varying the light intensity between 27.1 and 41.0 W m<sup>-2</sup>, corresponding to photonic fluxes of 0.34 and 0.44 J s<sup>-1</sup>, using the SUNTEST at 300 or 500, respectively [44], or using the natural sunlight with an intensity of 31.0 W m<sup>-2</sup>, corresponding to a photonic flux of 0.29 J s<sup>-1</sup>. The Cr(VI) reduction proved to be strongly depend on the irradiance source. Using the SUNTEST at 300 W m<sup>-2</sup> the Cr(VI) total reduction was achieved with an accumulated energy of 2.44 kJ L<sup>-1</sup>, while using the SUNTEST at 500 W m<sup>-2</sup>, the same reduction was achieved with 1.41 kJ L<sup>-1</sup> (Fig. 11). Regarding the Cr(VI) reduction using natural solar light in the same photoreactor, the total reduction was achieved with an accumulated energy of 1.93 kJ L<sup>-1</sup>, a result very close to the one obtained with SUNTEST at 300 W m<sup>-2</sup>. In fact, the UV intensity of the SUNTEST at 300 W m<sup>-2</sup> is very similar to the one observed with natural solar light in a sunny winter day, while the UV intensity of the SUNTEST at 500 W m<sup>-2</sup> is related to the one observed with natural solar light in a sunny summer day. These results emphasise, this way, the viability of using natural solar irradiation on the Cr(VI) reduction treatment by a TiO<sub>2</sub>/UVA-vis/citric acid system.

### 3.7. Effect of CAM reuse on the photocatalytic reduction of Cr(VI) by CAM-TiO<sub>2</sub>/UVA-vis/citric acid system

A final important aspect to consider is the ability for the immobilized TiO<sub>2</sub> to be reused. The reuse of the catalyst in a photocatalytic reaction would reduce the working cost of the system to a great extent, as well as the solid waste generation. This way, the CAM structures coated with 6 P25 thin layers were reused for 10 consecutive photocatalytic reduction cycles using fresh solutions of 0.02 mM of Cr(VI), 6.9 mM of citric acid, pH 2.5 and temperature of 25 °C. After each photocatalytic cycle, the CAM structures were washed with distilled water, dried at 50 °C for 30 min and weighed. The mass of the CAM structure did not change during the reuse experiments, indicating a negligible leaching of the nanoparticles to the solution and, consequently, the deposition method efficiency. Table 2 shows that despite the  $k$  and photonic efficiency values decreased at a ratio of 1.7 from the first to the second cycle, after that, the Cr(VI) photocatalytic reduction remained almost similar up to the 10th reduction cycle, achieving residual Cr(VI) concentrations, below the detection limit of the method, in a maximum of 90 min (Fig. 12). Kabra et al. [45] showed that using TiO<sub>2</sub> suspensions, the catalyst can be only used 2–3 times for lower Cr(VI) concentrations. On the other hand, Liu et al. [46] reported that TiO<sub>2</sub>-impregnated glutaraldehyde-crosslinked alginate beads can maintain full photoactivity for at least three Cr(VI) reduction cycles, emphasising the advantage of using an immobilized catalyst.

Since TiO<sub>2</sub> leaching from the CAM structure during the reuse cycles is negligible and the Cr(III) is not adsorbed on the film surface, a possible explanation for the loss of efficiency after the first cycle is the TiO<sub>2</sub> surface blocking by the citric acid or by its byproducts. In order to eliminate the possible organic products on the TiO<sub>2</sub> surface, another set of reuse tests with 2 cycles was performed to treat fresh

solutions of 0.02 mM of Cr(VI), 6.9 mM of citric acid, pH 2.5 and temperature of 25 °C. After the first cycle, the CAM-TiO<sub>2</sub> structures were maintained inside the reactor and washed two times over recirculation of 1.5 L of distilled water under irradiation throughout a total of 4 h, in order to mineralize all the organic compounds present in the catalyst surface. Since the absorbance of the slurry TiO<sub>2</sub> is detected even in small dosages at 500 nm (detection limit of 0.9 mg of TiO<sub>2</sub> nanoparticles per liter of solution) and the presence of Cr(VI), Cr(III) and citric acid does not interfere at this wavelength, in order to verify the presence of leached TiO<sub>2</sub>, samples were taken after each wash and during all the reaction time to measure the absorbance at 500 nm. However, no signal was observed in all samples, emphasising that almost no TiO<sub>2</sub> leaching occurred during the reaction. As it is possible to see at Fig. 13 similar results were observed in both first and second cycles ( $k = 46 \times 10^{-3} \text{ min}^{-1}$ ,  $\xi = 1.529\%$  and  $k = 48 \times 10^{-3} \text{ min}^{-1}$ ,  $\xi = 1.591\%$ , respectively), proving the hypothesis that citric acid and/or its byproducts can inactivate the TiO<sub>2</sub> thin film surface and those compounds must be removed when the CAM-TiO<sub>2</sub> reuse is intended. Several techniques have been tested by others authors for TiO<sub>2</sub> films reactivation after the organic compounds treatment, as washing with NaOH and NH<sub>4</sub>OH solutions, H<sub>2</sub>O<sub>2</sub>/UVC and calcination, being the H<sub>2</sub>O<sub>2</sub>/UVC and the calcination methods pointed as the most effective ones [47].

#### 4. Conclusions

Solar photocatalytic reduction of hexavalent chromium was successfully achieved using transparent cellulose acetate monolithic structures coated with TiO<sub>2</sub>-P25 in the presence of citric acid. The reaction kinetics and the photonic efficiency proved to depend on the TiO<sub>2</sub> amount immobilized on the CAM structures: the best results were attained with 6 P25 layers, value from which both parameters remain almost constant. The CAM structures provided a high surface area-to-volume ratio with an illuminated catalyst surface area per unit of reaction liquid volume inside the reactor of 212 m<sup>2</sup> m<sup>-3</sup>. A photocatalyst reactivity in combination with the photoreactor of 0.07 mmol<sub>Cr(VI)</sub> m<sup>-3</sup> illuminated volume s<sup>-1</sup> was achieved, corresponding to 152 mmol<sub>Cr(VI)</sub> m<sup>-3</sup> illuminated volume kJ<sup>-1</sup>.

The solution pH value showed to have an important effect on the Cr(VI) photocatalytic reduction rate: the more acidic the pH value, the higher the reduction rate. The increase of citric acid concentration enhanced significantly the Cr(VI) removal ([Cr]<sub>0</sub> = 0.02 mM), achieving the highest reduction rate using a concentration of 6.9 mM. It was also concluded that the citric acid concentration should be adjusted in proportion to the Cr(VI) initial concentration. The Cr(VI) photocatalytic reduction rates proved also to depend on the scavenger organic agent used: the maximum reduction rate was attained using citric acid, decreasing in the following order: citric acid > oxalic acid > EDTA > maleic acid. Finally, using a simple dip coating deposition method, the TiO<sub>2</sub>-P25 CAM structures showed an effective catalytic stability during 10 consecutive Cr(VI) reduction cycles.

#### Acknowledgments

This work was financially supported by: Project POCI-01-0145-FEDER-006984—Associate Laboratory LSRE-LCM funded by FEDER funds through COMPETE2020 — Programa Operacional Competitividade e Internacionalização (POCI) — and by national funds through FCT — Fundação para a Ciência e a Tecnologia. V.J.P. Vilar acknowledges the FCT Investigator 2013 Programme (IF/00273/2013). B.A. Marinho acknowledges Capes for her scholarship (BEX-0983-13-6). R.O. Cristóvão thanks FCT for her Post-doc Scholarship (SFRH/BPD/101456/2014). R. Djellabi acknowledges European Union for his Post-doctoral Scholarship (Erasmus

Mundus Programme, BATTUTA Project, Action 2—STRAND 1, Lot 1, North Africa Countries).

#### Appendix A. Supplementary data

Supplementary data associated with this article can be found, in the online version, at <http://dx.doi.org/10.1016/j.apcatb.2016.09.061>.

#### References

- [1] J.M. Meichtry, M. Brusa, G. Mailhot, M.A. Grela, M.I. Litter, Heterogeneous photocatalysis of Cr(VI) in the presence of citric acid over TiO<sub>2</sub> particles: relevance of Cr(V)—citrate complexes, *Appl. Catal. B: Environ.* 71 (2007) 101–107.
- [2] X. Lv, G. Jiang, X. Xue, D. Wu, T. Sheng, C. Sun, X. Xu, Fe<sup>0</sup>-Fe<sub>3</sub>O<sub>4</sub> nanocomposites embedded polyvinyl alcohol/sodium alginate beads for chromium (VI) removal, *J. Hazard. Mater.* 262 (2013) 748–758.
- [3] S.G. Schrank, H.J. José, R.F.P.M. Moreira, Simultaneous photocatalytic Cr(VI) reduction and dye oxidation in a TiO<sub>2</sub> slurry reactor, *J. Photochem. Photobiol. A: Chem.* 147 (2002) 71–76.
- [4] S. Chakrabarti, B. Chaudhuri, S. Bhattacharjee, A.K. Ray, B.K. Dutta, Photo-reduction of hexavalent chromium in aqueous solution in the presence of zinc oxide as semiconductor catalyst, *Chem. Eng. J.* 153 (2009) 86–93.
- [5] M. Celebi, M. Yurderi, A. Bulut, M. Kaya, M. Zahmakiran, Palladium nanoparticles supported on amine-functionalized SiO<sub>2</sub> for the catalytic hexavalent chromium reduction, *Appl. Catal. B: Environ.* 180 (2016) 53–64.
- [6] U. Baig, R.A.K. Rao, A.A. Khan, M.M. Sanagi, M.A. Gondal, Removal of carcinogenic hexavalent chromium from aqueous solutions using newly synthesized and characterized polypyrrrole-titanium(IV)phosphate nanocomposite, *Chem. Eng. J.* 280 (2015) 494–504.
- [7] Q. Wu, J. Zhao, G. Qin, C. Wang, X. Tong, S. Xue, Photocatalytic reduction of Cr(VI) with TiO<sub>2</sub> film under visible light, *Appl. Catal. B: Environ.* 142–143 (2013) 142–148.
- [8] G. Cappelletti, C.L. Bianchi, S. Ardizzone, Nano-titania assisted photoreduction of Cr(VI): the role of the different TiO<sub>2</sub> polymorphs, *Appl. Catal. B: Environ.* 78 (2008) 193–201.
- [9] J.J. Testa, M.A. Grela, M.I. Litter, Heterogeneous photocatalytic reduction of Chromium(VI) over TiO<sub>2</sub> particles in the presence of oxalate: involvement of Cr(V) species, *Environ. Sci. Technol.* 38 (2004) 1589–1594.
- [10] K.M. Joshi, V.S. Shrivastava, Photocatalytic degradation of Chromium (VI) from wastewater using nanomaterials like TiO<sub>2</sub>, ZnO, and CdS, *Appl. Nanosci.* 1 (2011) 147–155.
- [11] J. Ananpattarakchai, P. Kajitivichyanukul, Enhancement of chromium removal efficiency on adsorption and photocatalytic reduction using a bio-catalyst, titania-impregnated chitosan/xylan hybrid film, *J. Clean. Prod.* 130 (2016) 126–136.
- [12] A.I. Cardona, R. Candal, B. Sánchez, P. Ávila, M. Rebollar, TiO<sub>2</sub> on magnesium silicate monolith: effects of different preparation techniques on the photocatalytic oxidation of chlorinated hydrocarbons, *Energy* 29 (2004) 845–852.
- [13] G.S. Shephard, S. Stockenström, D. de Villiers, W.J. Engelbrecht, G.F.S. Wessels, Degradation of microcystin toxins in a falling film photocatalytic reactor with immobilized titanium dioxide catalyst, *Water Res.* 36 (2002) 140–146.
- [14] S. Akkan, İ. Altin, M. Koç, M. Sökmen, TiO<sub>2</sub> immobilized PCL for photocatalytic removal of hexavalent chromium from water, *Desalin. Water Treat.* 56 (2015) 2522–2531.
- [15] T. Van Gerven, G. Mul, J. Moulijn, A. Stankiewicz, A review of intensification of photocatalytic processes, *Chem. Eng. Process. Process Intensif.* 46 (2007) 781–789.
- [16] R.A.R. Monteiro, S.M. Miranda, V.J.P. Vilar, L.M. Pastrana-Martínez, P.B. Tavares, R.A.R. Boaventura, J.L. Faria, E. Pinto, A.M.T. Silva, N-modified TiO<sub>2</sub> photocatalytic activity towards diphenhydramine degradation and *Escherichia coli* inactivation in aqueous solutions, *Appl. Catal. B: Environ.* 162 (2015) 66–74.
- [17] H. Lin, K.T. Valsaraj, Development of an optical fiber monolith reactor for photocatalytic wastewater treatment, *J. Appl. Electrochem.* 35 (2005) 699–708.
- [18] L.X. Pinho, J. Azevedo, S.M. Miranda, J. Ângelo, A. Mendes, V.J.P. Vilar, V. Vasconcelos, R.A.R. Boaventura, Oxidation of microcystin-LR and cylindrospermopsin by heterogeneous photocatalysis using a tubular photoreactor packed with different TiO<sub>2</sub> coated supports, *Chem. Eng. J.* 266 (2015) 100–111.
- [19] R.A.R. Monteiro, S.M. Miranda, C. Rodrigues-Silva, J.L. Faria, A.M.T. Silva, R.A.R. Boaventura, V.J.P. Vilar, Gas phase oxidation of n-decane and PCE by photocatalysis using an annular photoreactor packed with a monolithic catalytic bed coated with P25 and PC500, *Appl. Catal. B: Environ.* 165 (2015) 306–315.
- [20] J.H.O.S. Pereira, A.C. Reis, O.C. Nunes, M.T. Borges, V.J.P. Vilar, R.A.R. Boaventura, Assessment of solar driven TiO<sub>2</sub>-assisted photocatalysis efficiency on amoxicillin degradation, *Environ. Sci. Pollut. Res.* 21 (2014) 1292–1303.

[21] K.L. Willett, R.A. Hites, Chemical actinometry: using *o*-nitrobenzaldehyde to measure lamp intensity in photochemical experiments, *J. Chem. Educ.* 77 (2000) 900.

[22] B.A. Marinho, R. Djellabi, R.O. Cristóvão, J.M. Loureiro, R.A.R. Boaventura, M.M. Dias, J.C.B. Lopes, V.J.P. Vilar, Intensification of heterogeneous  $\text{TiO}_2$  photocatalysis using an innovative micro-meso-structured-reactor for Cr(VI) reduction under simulated solar light, *Chem. Eng. J.* (in press).

[23] Y. Ku, I.-L. Jung, Photocatalytic reduction of Cr(VI) in aqueous solutions by UV irradiation with the presence of titanium dioxide, *Water Res.* 35 (2001) 135–142.

[24] P. Kajitvichyanukul, C.R. Chenthamarakshan, K. Rajeshwar, S.R. Qasim, Photocatalytic reactivity of thallium(I) species in aqueous suspensions of titania, *J. Electroanal. Chem.* 519 (2002) 25–32.

[25] D. Chen, F. Li, A.K. Ray, External and internal mass transfer effect on photocatalytic degradation, *Catal. Today* 66 (2001) 475–485.

[26] A. Mills, S. Le Hunte, An overview of semiconductor photocatalysis, *J. Photochem. Photobiol. A: Chem.* 108 (1997) 1–35.

[27] M.J. Lima, C.G. Silva, A.M.T. Silva, J.C.B. Lopes, M.M. Dias, J.L. Faria, Homogeneous and heterogeneous photo-fenton degradation of antibiotics using an innovative static mixer photoreactor, *Chem. Eng. J.* (in press).

[28] F.V.S. Lopes, S.M. Miranda, R.A.R. Monteiro, S.D.S. Martins, A.M.T. Silva, J.L. Faria, R.A.R. Boaventura, V.J.P. Vilar, Perchloroethylene gas-phase degradation over titania-coated transparent monoliths, *Appl. Catal. B: Environ.* 140–141 (2013) 444–456.

[29] C.D. Wagner, A.V. Naumkin, A. Kraut-Vass, J.W. Allison, C.J. Powell, J.R.J. Rumble, NIST Standard Reference Database 20, Version 4.1 (2012).

[30] J. Giménez, M.A. Aguado, S. Cervera-March, Photocatalytic reduction of chromium(VI) with titania powders in a flow system. Kinetics and catalyst activity, *J. Mol. Catal. A: Chem.* 105 (1996) 67–78.

[31] X. Wang, S.O. Pehkonen, A.K. Ray, Removal of aqueous Cr(VI) by a combination of photocatalytic reduction and coprecipitation, *Ind. Eng. Chem. Res.* 43 (2004) 1665–1672.

[32] Q. Cheng, C. Wang, K. Doudrick, C.K. Chan, Hexavalent chromium removal using metal oxide photocatalysts, *Appl. Catal. B: Environ.* 176–177 (2015) 740–748.

[33] Y. Di Iorio, E.S. Román, M.I. Litter, M.A. Grela, Photoinduced reactivity of strongly coupled  $\text{TiO}_2$  ligands under visible irradiation: an examination of an alizarin red@ $\text{TiO}_2$  nanoparticulate system, *J. Phys. Chem. C* 112 (2008) 16532–16538.

[34] S.M. Abdel Moniem, M.E.M. Ali, T.A. Gad-Allah, A.S.G. Khalil, M. Ulbricht, M.F. El-Shahat, A.M. Ashmawy, H.S. Ibrahim, Detoxification of hexavalent chromium in wastewater containing organic substances using simonkolleite- $\text{TiO}_2$  photocatalyst, *Process Saf. Environ. Prot.* 95 (2015) 247–254.

[35] A. Khan, N.A. Mir, M. Faisal, M. Muneer, Titanium dioxide-mediated photocatalysed degradation of two herbicide derivatives chlорidazon and metribuzin in aqueous suspensions, *Int. J. Chem. Eng.* 2012 (2012) 8.

[36] M. Hasmath Farzana, S. Meenakshi, Photocatalytic aptitude of titanium dioxide impregnated chitosan beads for the reduction of Cr(VI), *Int. J. Biol. Macromol.* 72 (2015) 1265–1271.

[37] F.V. Hackbarth, D. Maass, A.U. de Souza, V.J.P. Vilar, S.M.A.G.U. de Souza, Removal of hexavalent chromium from electroplating wastewaters using marine macroalgae *Pelvetia canaliculata* as natural electron donor, *Chem. Eng. J.* 290 (2016) 477–489.

[38] M.I. Litter, Heterogeneous photocatalysis: transition metal ions in photocatalytic systems, *Appl. Catal. B: Environ.* 23 (1999) 89–114.

[39] T. Aarthi, G. Madras, Photocatalytic reduction of metals in presence of combustion synthesized nano- $\text{TiO}_2$ , *Catal. Commun.* 9 (2008) 630–634.

[40] D. Chen, A.K. Ray, Removal of toxic metal ions from wastewater by semiconductor photocatalysis, *Chem. Eng. Sci.* 56 (2001) 1561–1570.

[41] N. Wang, L. Zhu, K. Deng, Y. She, Y. Yu, H. Tang, Visible light photocatalytic reduction of Cr(VI) on  $\text{TiO}_2$  in situ modified with small molecular weight organic acids, *Appl. Catal. B: Environ.* 95 (2010) 400–407.

[42] M.I. Franch, J.A. Ayllón, J. Peral, X. Domènec, Photocatalytic degradation of short-chain organic diacids, *Catal. Today* 76 (2002) 221–233.

[43] Y.-C. Oh, X. Li, J.W. Cabbage, W.S. Jenks, Mechanisms of catalyst action in the  $\text{TiO}_2$ -mediated photocatalytic degradation and cis-trans isomerization of maleic and fumaric acid, *Appl. Catal. B: Environ.* 54 (2004) 105–114.

[44] B.A. Marinho, R.O. Cristóvão, J.M. Loureiro, R.A.R. Boaventura, V.J.P. Vilar, Solar photocatalytic reduction of Cr(VI) over Fe(III) in the presence of organic sacrificial agents, *Appl. Catal. B: Environ.* 192 (2016) 208–219.

[45] K. Kabra, R. Chaudhary, R.L. Sawhney, Photocatalytic reduction of Cr(VI) in aqueous titania suspensions exposed to concentrated solar radiation, *Int. J. Sustainable Energy* 26 (2007) 195–207.

[46] Y.-G. Liu, X.-J. Hu, H. Wang, A.-W. Chen, S.-M. Liu, Y.-M. Guo, Y. He, X. Hu, J. Li, S.-H. Liu, Y.-Q. Wang, L. Zhou, Photoreduction of Cr(VI) from acidic aqueous solution using  $\text{TiO}_2$ -impregnated glutaraldehyde-crosslinked alginate beads and the effects of Fe(III) ions, *Chem. Eng. J.* 226 (2013) 131–138.

[47] N. Miranda-García, S. Suárez, M.I. Maldonado, S. Malato, B. Sánchez, Regeneration approaches for  $\text{TiO}_2$  immobilized photocatalyst used in the elimination of emerging contaminants in water, *Catal. Today* 230 (2014) 27–34.